Stretch-induced Calcium Release in Smooth Muscle

Guangju Ji,[1] Robert J. Barsotti,[2] Morris E. Feldman,[1] and Michael I. Kotlikoff[1]

[1]Department of Biomedical Sciences College of Veterinary Medicine Cornell University, Ithaca, NY 14853

[2]Department of Pathology, Anatomy, and Cell Biology Jefferson Medical College, Thomas Jefferson University, Philadelphia, PA 19107

ABSTRACT Smooth muscle cells undergo substantial increases in length, passively stretching during increases in intraluminal pressure in vessels and hollow organs. Active contractile responses to counteract increased transmural pressure were first described almost a century ago (Bayliss, 1902) and several mechanisms have been advanced to explain this phenomenon. We report here that elongation of smooth muscle cells results in ryanodine receptor–mediated Ca^{2+} release in individual myocytes. Mechanical elongation of isolated, single urinary bladder myocytes to ~120% of slack length ($\Delta L = 20$) evoked Ca^{2+} release from intracellular stores in the form of single Ca^{2+} sparks and propagated Ca^{2+} waves. Ca^{2+} release was not due to calcium-induced calcium release, as release was observed in Ca^{2+}-free extracellular solution and when free Ca^{2+} ions in the cytosol were strongly buffered to prevent increases in $[Ca^{2+}]_i$. Stretch-induced calcium release (SICR) was not affected by inhibition of $InsP_3R$-mediated Ca^{2+} release, but was completely blocked by ryanodine. Release occurred in the absence of previously reported stretch-activated currents; however, SICR evoked calcium-activated chloride currents in the form of transient inward currents, suggesting a regulatory mechanism for the generation of spontaneous currents in smooth muscle. SICR was also observed in individual myocytes during stretch of intact urinary bladder smooth muscle segments. Thus, longitudinal stretch of smooth muscle cells induces Ca^{2+} release through gating of RYR. SICR may be an important component of the physiological response to increases in luminal pressure in smooth muscle tissues.

KEY WORDS: ryanodine receptor • Ca^{2+} sparks • calcium-activated chloride current • cation current • sarcoplasmic reticulum

INTRODUCTION

Calcium release from the sarcoplasmic reticulum (SR)* of muscle is a highly developed process involving the coupling of signals at the sarcolemma to the gating of SR Ca^{2+} release channels. Thus, in skeletal and cardiac muscle, depolarization of the sarcolemma triggers the opening of ryanodine receptors (RYRs) either through a physical association between the L-type Ca^{2+} channel and RYR1 (Tanabe et al., 1988; Tanabe et al., 1990; Nakai et al., 1998) or a rise in $[Ca^{2+}]_i$ in the microdomain of the L-type channel, which is sensed by RYR2 resulting in calcium-induced calcium release (CICR) (Fabiato, 1983; Nabauer et al., 1989; Cannell et al., 1995; Lopez-Lopez et al., 1995; Lipp and Niggli, 1996; Collier et al., 1999). In smooth muscle, biochemical coupling between phospholipase C–linked receptors and $InsP_3$ receptor ($InsP_3R$) Ca^{2+} channels on the SR serves an analogous function in excitation–contraction coupling (Baron et al., 1984; Somlyo et al., 1985, 1988). However, despite the presence of a well developed $InsP_3$-coupled Ca^{2+} release system, RYR-mediated Ca^{2+} release has been demonstrated in several forms in smooth muscle (Ganitkevich and Isenberg, 1992; Nelson et al., 1995; Imaizumi et al., 1998; Collier et al., 2000). This release process takes the form of spontaneous Ca^{2+} sparks (Nelson et al., 1995) in nonspiking myocytes and CICR in urinary bladder myocytes (Collier et al., 2000). In fact, both processes likely involve CICR in that the probability of opening of RYR channels is a function of $[Ca^{2+}]_i$. Thus, in spiking myocytes, the opening of L-type Ca^{2+} channels during the action potential results in a rise in $[Ca^{2+}]_i$, which increases the probability of release in the form of unitary Ca^{2+} sparks (Collier et al., 2000). Such a process is analogous to the spontaneous calcium release events observed in sarcomeric muscle (Klein et al., 1996).

In many smooth muscle tissues, individual myocytes are exposed to considerable mechanical stress and associated changes in cell length and it has long been known that increases in passive tension evoke contraction of smooth muscle (Bayliss, 1902). One process by which mechanical stress may couple to cellular activation is through the opening of mechano or stretch-sensitive ion channels (Guharay and Sachs, 1984; Sigurdson et al., 1992). Stretch-activated cation channels have been reported in smooth muscle and may promote E-C coupling by depolarizing myocytes and by mediating sufficient Ca^{2+} flux to effect contraction (Kirber et al.,

---

Address correspondence to Michael I. Kotlikoff, Department of Biomedical Sciences, College of Veterinary Medicine, Cornell University, T4018 VRT, Box 11, Ithaca, NY 14853-6401. Fax: (607) 253-3317; E-mail: mik7@cornell.edu

*Abbreviations used in this paper: CICR, calcium-induced calcium release; RYR, ryanodine receptor; SICR, stretch-induced calcium release; SR, sarcoplasmic reticulum; STIC, spontaneous inward current.

1988; Wellner and Isenberg, 1993a, 1994). Moreover, Ca^{2+} influx through these channels may be amplified through CICR (Kirber et al., 2000). We reasoned that alterations in cell length could trigger CICR in smooth muscle through the activation of stretch-activated cation channels and designed experiments to examine this possibility. Here we demonstrate that increases in cell length result in the gating of RYR and the release of Ca^{2+} from the SR in the form of Ca^{2+} sparks or propagated Ca^{2+} waves, depending on the degree of cell stretch. However, this process does not require an influx of extracellular Ca^{2+} ions, activation of ionic currents, or even a rise in $[Ca^{2+}]_i$. Thus, stretch-induced calcium release (SICR) may constitute an additional form of coupling between the sarcolemma and the SR.

MATERIALS AND METHODS

Cell Isolation

Rabbits and mice were anesthetized and killed in accordance with an approved laboratory animal protocol. Single rabbit cells were prepared as described previously (Collier et al., 2000). Briefly, the urinary bladder was removed, dissected in ice-cold oxygenated physiological salt solution, minced, and suspended in modified 1.5 mg/ml collagenase type II (Worthington Biochemical), 1 mg/ml protease type XIV, and 5 mg/ml bovine serum albumin (Sigma-Aldrich) at 37°C for 35–40 min. Mouse bladder myocytes were isolated by cutting the bladder into small pieces, which were then incubated for 20 min in 1 mg/ml papain, 1 mg/ml dithioerythritol, and 1 mg/ml bovine serum albumin Ca^{2+}-free solution (see below). The fragments were then transferred into 1 mg/ml collagenase type II and 100 μM Ca^{2+} solution supplemented with 1 mg/ml bovine serum albumin and incubated for 10 min, then triturated with a wide-bore Pasteur pipette, and passed through 125-μm nylon mesh. Cells were concentrated by low speed centrifugation, washed with fresh medium, resuspended, and stored at 4°C.

Tissue Preparation

For imaging of isolated bladder tissues, the mouse bladder was removed and the fibrosal and mucosal layers dissected away in ice-cold Ca^{2+} free solution. Muscle segments, 2–3 mm in length and 100–200 μm in diameter, were cut using a fine dissecting scissors. Each end of the strip was trimmed, wrapped in T-shaped aluminum clips, and gently digested in 0.5 mg/ml collagenase type II with 1 mg/ml bovine serum albumin for 5 min at 32°C.

Measurement of Ca^{2+} Fluorescence

Single myocytes were incubated with 10 μM Fluo-4 a.m. (Molecular Probes) for 10 min at room temperature in a recording chamber mounted on an inverted microscope (TE300; Nikon) and perfused with physiological salt extracellular solution for 40 min at room temperature. The extracellular solution was (mM): 140 NaCl, 5.4 KCl, 1.8 $CaCl_2$, 1.2 $MgCl_2$, 10 HEPES, and 10 glucose (pH 7.4, adjusted with NaOH). For the Ca^{2+}-free extracellular solution, $CaCl_2$ was omitted from the above solution or 3 mM EGTA and 1 mM $CaCl_2$ was used to clamp free $[Ca^{2+}]$ at ~100 nM, as indicated. Solutions were changed using a gravity perfusion system providing complete solution exchange within 30 s. Cell stretch was accomplished using two patch pipettes attached

to separate manipulators, and tip-loaded with Fluo-4 pentapotassium salt to facilitate detection of the degree of stretch. Pipettes were sealed to cells either by suction to form a high resistance seal, or by coating the pipette tip with polyurathane foam (Great Stuff; Flexible Products Co.). Cells were stretched by moving the pipettes along the longitudinal cell axis; stretch from slack length (L_1) to a new length (L_2) is reported as the percent increase in cell length, or $(L_2 - L_1)/L_1$. For experiments in tissue segments, the preparations were incubated with Fluo-4 a.m. (10 μM) and 0.05% pluronic acid for 1 h and transferred via a fine glass rod to a 60-μl solution trough mounted on the inverted microscope. The T-clips were placed over fine wire hooks to suspend the preparation and the segments were lowered to the bottom of the trough, which was made from a thin quartz coverslip. The strip was initially stretched by a few percent over slack length to approximate resting length. All experiments were performed at room temperature.

Fluo-4 fluorescence was recorded using a laser scanning confocal head (Radiance 2000; BioRad Laboratories) attached to an inverted microscope (TE-300; Nikon) with a plan-apo 60× water immersion objective (1.2 n.a.; Nikon). Cells were excited with 488 nm light from a krypton/argon laser and linescan or x-y images recorded using Lasersharp software (Bio-Rad Laboratories). Linescans were obtained at an interval of 1.33 or 0.833 ms per line; x-y images (128 pixels × 30 or 40 lines) were recorded at an average frame rate of 37.5-, 44-, or 57.3-ms intervals. Images were analyzed using LaserPix version 4.2 software (Bio-Rad Laboratories). Fluorescence profiles were constructed from x-y and linescan images using LaserPix or custom developed software. For x-y images a mean baseline fluorescence intensity (F_0) was obtained by averaging a quiescent area of the cell (four or five pixel diameter) for the first 20 images. A three pixel diameter area of interest was centered on a Ca^{2+} spark and the average value (F) of that area divided by F_0 on a frame-by-frame basis. For linescan images, F_0 was obtained by averaging the fluorescence for each pixel (x dimension) for a period preceding activation of a Ca^{2+} spark, and the fluorescence of all pixels (F) was divided by F_0. Profiles were constructed by averaging three pixels bisecting a Ca^{2+} spark for each time point in the scan.

Patch-Clamp Recording

Membrane currents were recorded during single-cell stretch experiments using whole-cell voltage clamp methods. In these experiments, one of the two stretching pipettes also served as a recording pipette and was filled with intracellular solution; after seals were formed at both ends, the membrane patch was ruptured in the recording pipette and cell lengthening was achieved by moving the nonrecording pipette. The intracellular solution was (mM): 130 CsCl, 1 $MgCl_2$, 10 Hepes, 0.075 EGTA, 1 Mg-ATP (pH = 7.2, adjusted with CsOH), and a seal formed in the middle of the cell. In some experiments high concentrations of mobile calcium buffer were used to clamp $[Ca^{2+}]_i$; in these experiments the above solution contained 17 mM EGTA with $CaCl_2$ adjusted to fix $[Ca^{2+}]_i$ at either 100 nM (7 mM $CaCl_2$) or <10 nM (1 mM $CaCl_2$), as determined using the WINCMAXC program (Chris Patton, Stanford University, Stanford, CA). The extracellular solution used in the membrane current recording was the same as described above. 100 mM NaCl was replaced by an equimolar amount of sodium glutamate to examine current selectivity. Currents were recorded in the whole-cell configuration; cells were clamped at −60 mV and voltage protocols imposed using an Axopatch 200 B amplifier and pCLAMP software (Axon Instruments, Inc.). The current reversal potential were measured by a ramp (from −80 to 80 mV) depolarization protocol; currents were not corrected for leakage.

Stretch Induces Ca²⁺ Sparks and Ca²⁺ Waves in Single Smooth Muscle Cells from the Urinary Bladder

Stretch Induces Ca^{2+} Sparks and Ca^{2+} Waves in Single Smooth Muscle Cells from the Urinary Bladder

To examine the effect of cell length on intracellular Ca^{2+} release, we examined Fluo-4 fluorescence in single myocytes by confocal microscopy during and after changes in cell length achieved by moving a pipette attached to one end of the cell along the long axis of the cell. As shown in Fig. 1 A, elongation of a rabbit urinary bladder myocyte by ∼20% of resting length typically evoked a series of Ca^{2+} sparks observed in a

time series (x-y) of images obtained every 40 ms. In 47 experiments of this kind (26 rabbit and 21 mouse bladder myocytes), Ca^{2+} sparks or waves were observed in 35 (75%) cells. Unitary Ca^{2+} sparks were similar in amplitude and time course to previous reports (Nelson et al., 1995; ZhuGe et al., 1998; Bolton and Gordienko, 1998; Collier et al., 2000) (Table I) and Ca^{2+} sparks occurred repeatedly at the same cell area or areas (Fig. 1 A), the so-called frequent discharge sites that have been reported for spontaneous Ca^{2+} sparks (Gordienko et al., 1998, 2001). Although spontaneous Ca^{2+} sparks are quite infrequent in rest-
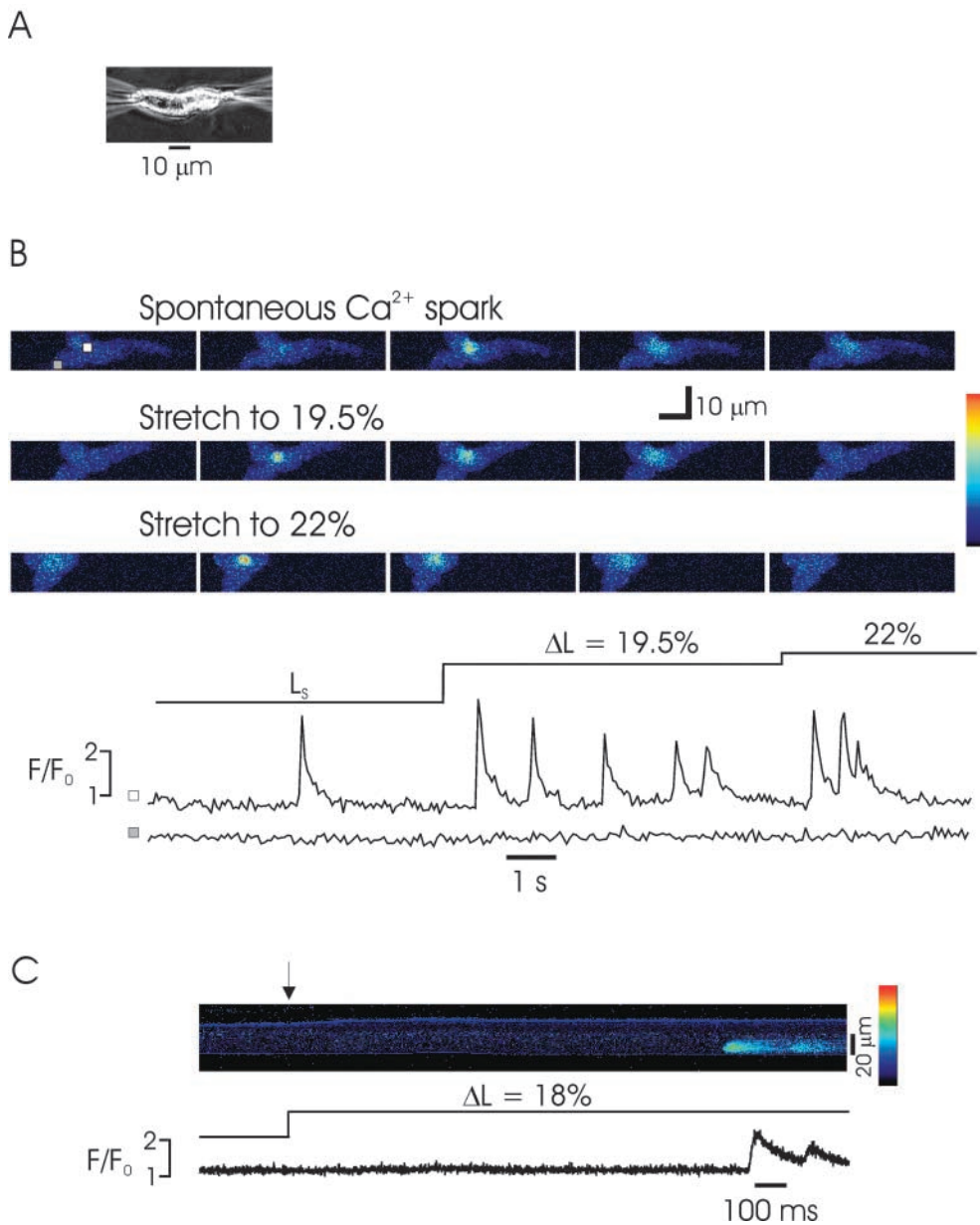

FIGURE 1. Stretch induces Ca^{2+} sparks in single rabbit urinary bladder myocytes. (A) Above, sequential confocal images obtained during a spontaneous Ca^{2+} spark (top), and after stretch-induced Ca^{2+} sparks after sequential stretch to ∼19.5 and 22% of cell length. Note that the Ca^{2+} sparks initiate from the same area of the cell and are of similar time course and amplitude. The cell position shifts following each elongation. Images were obtained at 57.3-ms intervals (pixel size 0.30 µM). The color bar at right indicates the pseudo-color representation of the minimum and maximum pixel values. The boxes in the first image indicate the area in which the pixel values were averaged from all images for the fluorescence profile (below). Below, the fluorescence profile (F/F_0) indicates the generation of multiple Ca^{2+} sparks in the same area (white box), whereas no increase is detected in another region of the cell (gray box). The images above correspond to the spontaneous Ca^{2+} spark and the first sparks after each stretch. The fluorescence profile was obtained by dividing the pixels in the area shown by the average cellular fluorescence under resting conditions (no Ca^{2+} sparks). ΔL indicates the extent of stretch $[(L_2 - Ls)/Ls]$, where L_s is the slack length of the cell. (B) Linescan image obtained before and during stretch of a myocyte shows two Ca^{2+} sparks arising from the same location shortly after the cell was stretched (arrow). The image was obtained at an interval of 1.33 ms/line (pixel size 0.50 µM). The fluorescence profile from the linescan is shown below.

TABLE I

Kinetics of Stretch-induced Ca^{2+} Sparks in Rabbit and Mouse Bladder Myocytes

Rise time	Decay ($t_{1/2}$)	FWHM	F/Fo
ms	*ms*	*μm*	
32.9 ± 3.3	66.8 ± 11.3	2.11 ± 1.33	1.54 ± 0.15
$n = 8$	$n = 8$	$n = 34$	$n = 26$

FWHM, full width half max.

ing urinary bladder myocytes (Collier et al., 2000), occasionally as shown in Fig. 1 A, spontaneous Ca^{2+} sparks and stretch-induced Ca^{2+} sparks could be observed in the same cell, allowing us to observe that they initiate from the same subcellular region. Ca^{2+} sparks were observed to occur repeatedly in elongated cells while the cells were at the new length ($\sim$10 s), although a prominent decay in activity occurred during this time (see below); following return to resting length Ca^{2+} spark frequency returned to baseline. The phenomenon of stretch-induced Ca^{2+} sparks was quite repeatable. In some cells tested, cell stretch evoked Ca^{2+} waves that propagated throughout the cell; stretch-induced Ca^{2+} waves propagated at a speed similar to previously reported Ca^{2+} waves evoked by CICR (Collier et al., 2000). As observed previously, the time course of Ca^{2+} sparks varied substantially based on the size of the underlying release event; that is, larger events that were locally propagated as Ca^{2+} waves had a substantially longer decay halftime than smaller, nonpropagating events.

Ca^{2+} sparks were also measured in linescan (x-t) mode to more accurately determine kinetics of Ca^{2+} sparks activated by stretch and to assess the average time delay between the onset of stretch and Ca^{2+} release (Fig. 1 B). As in time series measurements, cell elongation resulted in one or more Ca^{2+} sparks. In these experiments, in which cells were stretched by a single, brief movement of the manipulator, the delay between the onset of mechanical stretch and the first Ca^{2+} spark was 2.15 ± 0.48 s ($n = 11$). Mean parameters for discrete Ca^{2+} sparks observed in linescan measurements are listed in Table I.

The pattern of Ca^{2+} release during cell elongation was also examined. Step increases in cell length were imposed to determine if Ca^{2+} release was sustained or accommodated, and whether Ca^{2+} release could be repeatedly obtained with subsequently imposed changes in cell length. Fig. 2 shows the fluorescence profiles from several experiments of this kind in which the degree and duration of length changes was varied. These experiments demonstrated that Ca^{2+} release was not sustained in time, but accommodated gradually during sustained cell stretch (A and B). This process did not result from a loss of Ca^{2+} from the SR or a com-
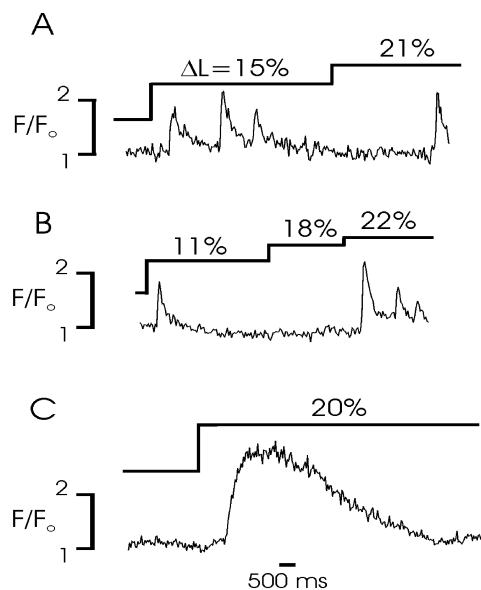

FIGURE 2. Pattern of Ca^{2+} release during repeated and sustained cell stretch. A–C show fluorescent profiles from x-y confocal images taken at 37.5-ms intervals; mouse myocytes were progressively stretched from slack length as shown. (A) An initial stretch elicits a burst of individual Ca^{2+} sparks from the same area of a cell; the sparks are not sustained, despite maintenance of the stretch. Further lengthening of the cell elicits an additional spark, indicating that the desensitization of the process does not reflect a loss of SR Ca^{2+}. (B) Initial stretch results in a single Ca^{2+} spark. An additional stretch does not activate a spark, but further elongation results in multiple Ca^{2+} sparks of declining amplitude from the same site. (C) A large sustained stretch results in a Ca^{2+} wave that propagates across the cell, resulting in a sustained increase in the local Ca^{2+} profile.

plete inactivation of the underlying release process; however, since subsequent increases in cell length always resulted in additional Ca^{2+} release. Two possibilities could account for this pattern. First, the sensed mechanical parameter may be the change in cell length, rather than absolute tension, resulting in gating of release only during the initial phase of a step change in length. The substantial delay in some release events relative to the length change, however, seems to argue against such a mechanism. Moreover, the increased Ca^{2+} release with additional increases in cell length observed in some experiments (e.g., B and C) would suggest that the amount of Ca^{2+} release is related to wall tension. An alternative explanation for the prominent observed desensitization is that the probability of gating of Ca^{2+} release channels is a function of cell length and there is an inherent inactivation process for gated channels, such that a fraction of available channels are gated by the initial stretch (which inactivate) and others by subsequent increases in cell length, resulting in an accommodation of Ca^{2+} release at any given length.

Stretch-induced Ca^{2+} Sparks Are Independent of Ca^{2+} Entry

Our previous experiments (Collier et al., 2000) indicated that L-type Ca^{2+} channels are loosely coupled to RYRs through an increase in global [Ca^{2+}], resulting in a modified form of CICR in smooth muscle. We hypothesized that passive increases in cell length result in an increase in [Ca^{2+}]$_i$ and CICR. Thus, despite the fact that measurements of global [Ca^{2+}]$_i$ did not indicate a rise in [Ca^{2+}]$_i$, we thought it likely that small increases in [Ca^{2+}]$_i$ associated with the opening of stretch-activated Ca^{2+} channels (Kirber et al., 1988; Wellner and Isenberg, 1993a, 1993b) might not be detected in Ca^{2+} imaging experiments. We designed several experiments to test this hypothesis (Fig. 3). First, cells were examined in Ca^{2+}-free extracellular solution to determine the dependence of the process on extracellular Ca^{2+} influx. Ca^{2+} sparks were triggered by cell stretch even in the absence of extracellular Ca^{2+} in 16 cells (11 rabbit, 5 mouse), indicating that the stimulus for release was likely not Ca^{2+} influx through stretch-activated cation channels. Moreover, similar results were obtained with free Ca^{2+} in the extracellular bath clamped at 100 nM using EGTA in seven experiments (four rabbit, three mouse), as shown in Fig. 3 A. Second, experiments were performed in the presence of Gd^{3+}, which has been shown to block these channels. Ca^{2+} sparks were activated by cell stretch in the presence of Gd^{3+} and no difference was observed in the probability of stretch-activated Ca^{2+} release (see Fig. 5 A). SICR was observed in five out of eight such experiments (3/5 mouse and 2/3 rabbit). Third, we performed simultaneous imaging and voltage-clamp experiments to determine whether nonselective currents were activated by cell stretch. No ionic currents preceded stretch-activated Ca^{2+} sparks or waves, although prominent calcium-induced chloride currents were observed during these events (Fig. 3 B, see below). We did not observe any stretch-induced cation currents in experiments on rabbit or mouse myocytes, which may indicate a species difference relative to previous reports of these currents in bladder smooth muscle (Wellner and Isenberg, 1994). Finally, a series of experiments were performed under intracellular Ca^{2+} buffering conditions that disrupt CICR (Collier et al., 2000). We reasoned that an augmentation of [Ca^{2+}]$_i$ might occur by one of several mechanisms when cells are stretched, resulting in a modified form of CICR. However, prevention of such a rise in [Ca^{2+}]$_i$ by dialysis with high buffering capacity solution (17 mM EGTA, [Ca^{2+}]$_i$ clamped at ~100 nM) did not inhibit stretch-induced Ca^{2+} release (Fig. 3 B). In these experiments, stretch was initiated 30 s after rupture of the membrane patch to prevent depletion of SR Ca^{2+} stores; dialysis with EGTA prevents a rise in global [Ca^{2+}]$_i$, but the excess Ca^{2+} buffer does not completely buffer local Ca^{2+} increases
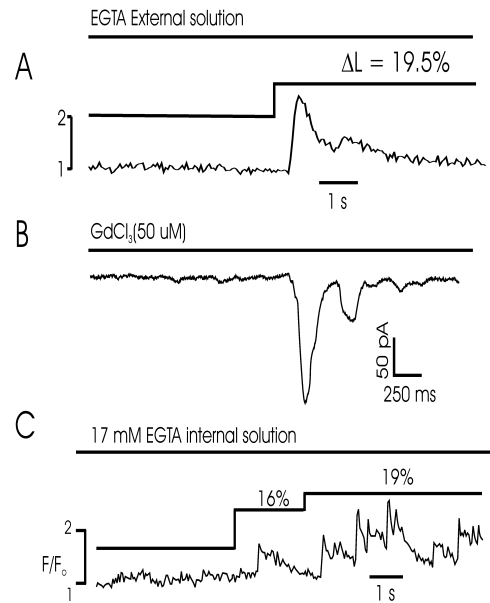

FIGURE 3. Stretch-induced Ca^{2+} release does not require Ca^{2+} entry or a rise in [Ca^{2+}]$_i$. (A) Fluorescence profile from a series of confocal images of a mouse myocyte indicates that stretch results in a Ca^{2+} wave in a cell perfused with Ca^{2+}-free extracellular solution. (B) Stretch-induced Ca^{2+} sparks/waves trigger inward currents in the presence of 50 μM GdCl$_3$ in a mouse myocyte, which blocks stretch-activated nonselective cation channels. The cell was stretched shortly before activation of the inward currents, which are calcium-activated chloride currents and indicate Ca^{2+} release (see Fig. 5). (C) Fluorescence profile obtained from a mouse cell dialyzed with 17 mM EGTA internal solution ([Ca^{2+}]$_i$ clamped at 100 nM). Repeated Ca^{2+} release events were observed following cell stretch in the presence of 17 mM mobile Ca^{2+} buffer. Equivalent results were obtained with [Ca^{2+}]$_i$ clamped to <5 nM.

near release sites, allowing detection by the Ca^{2+} indicator (Collier et al., 2000). Although [Ca^{2+}]$_i$ is not completely clamped under these conditions (since brief, spatially restricted increases are observed), this experiment mimics those which disrupt coupling between I$_{Ca}$ and Ca^{2+} release (Collier et al., 2000), further indicating that stretch-activated Ca^{2+} release is independent of extracellular Ca^{2+} influx and does not require a global increase in [Ca^{2+}]$_i$. In additional experiments (unpublished data), we observed SICR in cells dialyzed with 17 mM EGTA internal solution and [Ca^{2+}]$_i$ clamped at <5 nM. These latter experiments suggest that SICR is not likely to occur through an increase in sensitivity of the CICR system to Ca^{2+}, since buffering [Ca^{2+}]$_i$ to very low values did not inhibit Ca^{2+} release.

Stretch-induced Ca^{2+} Release Is Associated with RYR Gating

Ca^{2+} release from the SR in smooth muscle is mediated by two intracellular calcium channels: inositol trisphosphate receptor (InsP$_3$R) and RYR channels. Both of these tetrameric channel complexes are Ca^{2+} sensitive
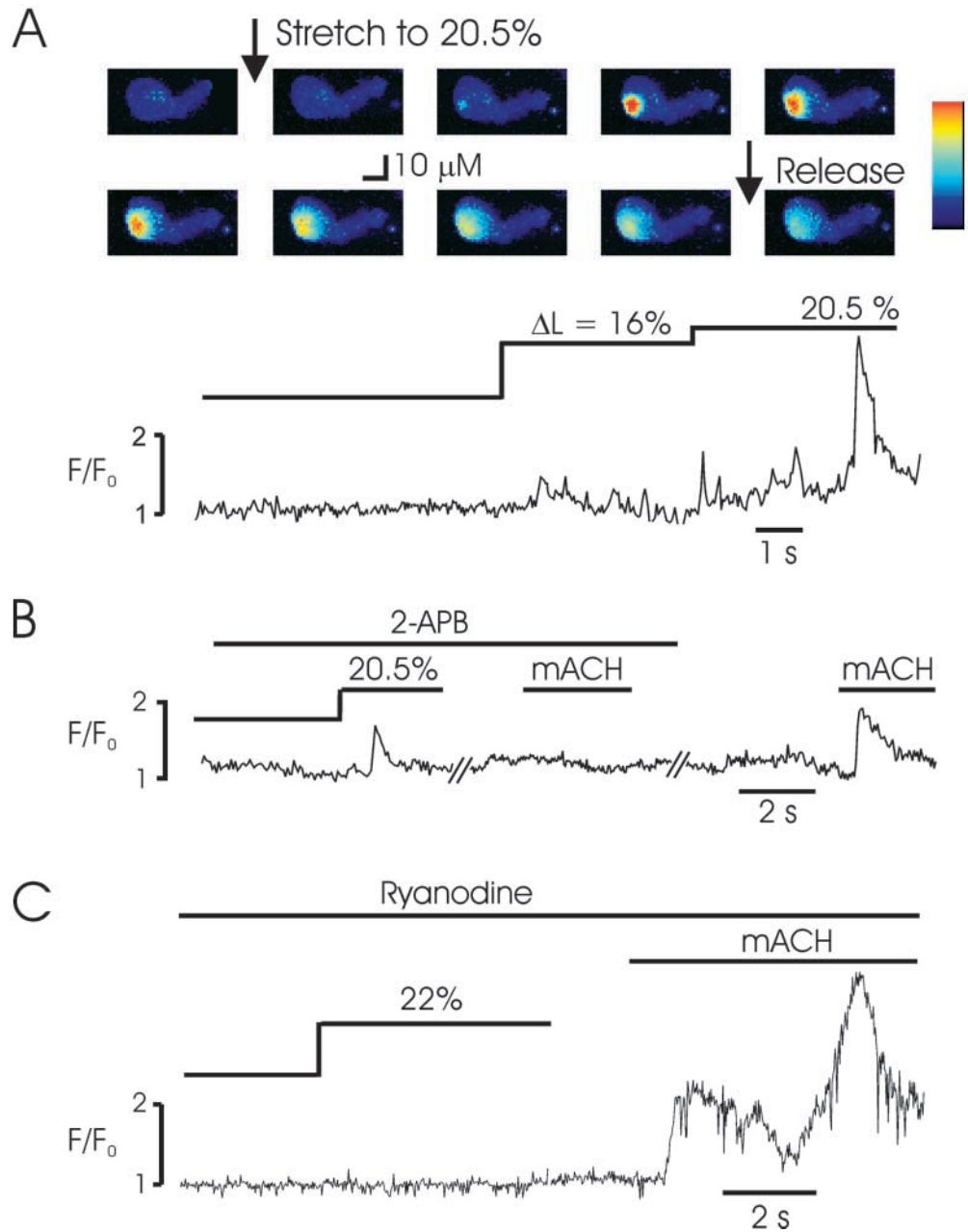
FIGURE 4. Stretch-induced Ca^{2+} release occurs through RYR gating. (A) Control experiment demonstrating a stretch-activated Ca^{2+} wave following cell stretch. Images shown are before, during, and after the second stretch of a mouse bladder myocyte. The fluorescence profile from the region of the initiation of the Ca^{2+} wave is shown for the entire experiment below. Pixel size = 0.95 μM. (B) Similar experiment in a mouse cell incubated with 2-APB (100 μM) to inhibit $InsP_3R$ demonstrates SICR in the form of Ca^{2+} sparks, despite the complete block of Ca^{2+} release by methacholine (mACH, 50 μM), indicating sufficient $InsP_3R$ block. (C) Incubation with ryanodine (10 μM) abolished SICR in a rabbit myocyte and this effect was not due to SR depletion, since methacholine was capable of releasing Ca^{2+}.

and can support local (Ca^{2+} sparks and puffs) and spatially transmitted (Ca^{2+} waves) signaling (Berridge, 1997). To determine whether SICR is associated with gating of $InsP_3R$ or RYR, we used inhibitors of each receptor and determined whether SICR was present. Fig. 4 B shows an example of a total of 15 experiments (nine in rabbit, six in mouse) demonstrating that following incubation of myocytes with 10 μM ryanodine for 30 min, cell stretch failed to induce Ca^{2+} sparks, although exposure of cells to mACH resulted in Ca^{2+} release. Conversely, SICR was not inhibited by incubation of cells with 2-APB (20 or 100 μM for 1 h), an $InsP_3$ receptor–selective antagonist (Fig. 4 C). Equivalent results were obtained in 11 rabbit and 4 mouse myocytes,

whereas 2-APB completely inhibited muscarinic Ca^{2+} release (Fig. 4 C). These data, as well as the amplitude and kinetics of stretch-induced Ca^{2+} sparks (Table I), indicate that myocyte stretch results in gating of RYR and the production of Ca^{2+} sparks similar to spontaneous events (Nelson et al., 1995; Gordienko et al., 1998; ZhuGe et al., 1998) or activated by CICR (Collier et al., 2000).

SICR Activates STICs and Macroscopic Ca^{2+}-activated Chloride Currents

Ca^{2+} sparks couple to the activation of sarcolemmal, calcium-activated potassium (Nelson et al., 1995), and chloride (ZhuGe et al., 1998) currents, and
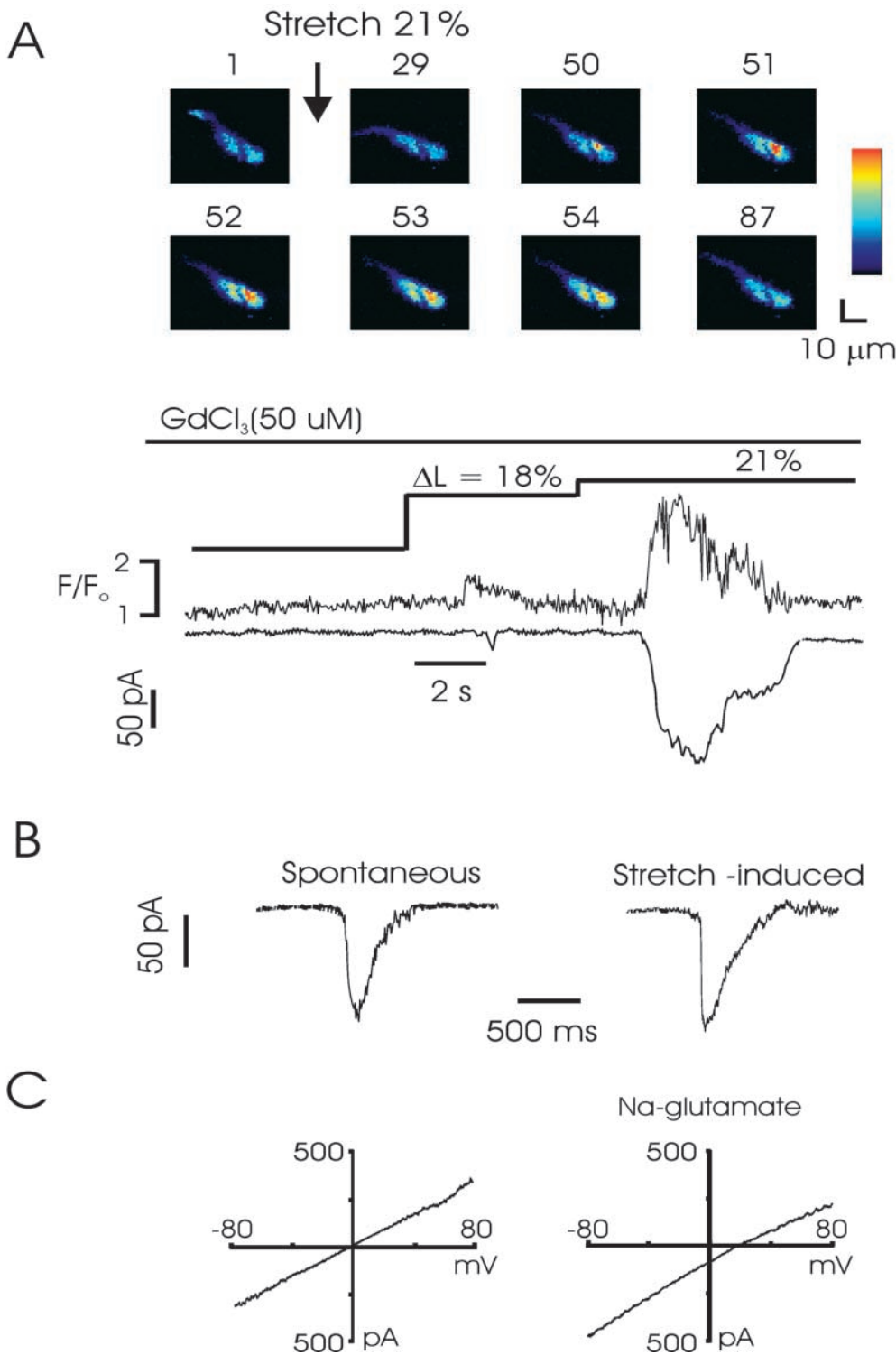
FIGURE 5. Stretch-induced Ca^{2+} release activates STICs and macroscopic Ca^{2+}-activated chloride currents. (A) Combined confocal and patch-clamp recording from a rabbit myocyte shows that SICR activates inward currents temporally and quantitatively linked to the Ca^{2+} release. The experiment was performed in the presence of Gd^{3+} (50 μM), which blocks stretch-activated cation currents. The numbers above each image indicate the relative timing of acquisition, beginning just before the stretch to 21%. Images were obtained every 44 ms. Pixel size = 1 μM. (B) Transient inward currents associated with calcium-activated chloride channel gating. Current at left occurred spontaneously, whereas current at right was evoked following cell stretch. Note roughly similar amplitude and kinetics. (C) I-V curve obtained from a ramp from −80 to 80 mV from a holding potential of −60 mV during stretch. Leak currents from ramp obtained before stretch have been subtracted. In physiological salt solution (left), stretch induces a linear current with a reversal potential of ~0, the equilibrium potential for Cl$^-$. Partial replacement of chloride with the poorly permeant anion glutamate shifts the reversal potential to ~18 mV, close to the theoretical Cl$^-$ reversal potential of 24 mV (right).

Ca^{2+} waves generate associated macroscopic currents (Collier et al., 2000). We next examined the activation of calcium-activated chloride currents in experiments using simultaneous recordings of membrane current and confocal fluorescence in stretched, voltage-clamped myocytes. In these experiments, one patch pipette was tip-filled with fluo-4 and sealed to the end of the cell for use as the "stretch" pipette and a second, recording, pipette was sealed near the middle of the cell and used in the whole-cell mode. Cell stretch consistently evoked inward currents that developed with a time course equivalent to the observed Ca^{2+} release; currents varied from very short, transient currents similar to spontaneous inward currents
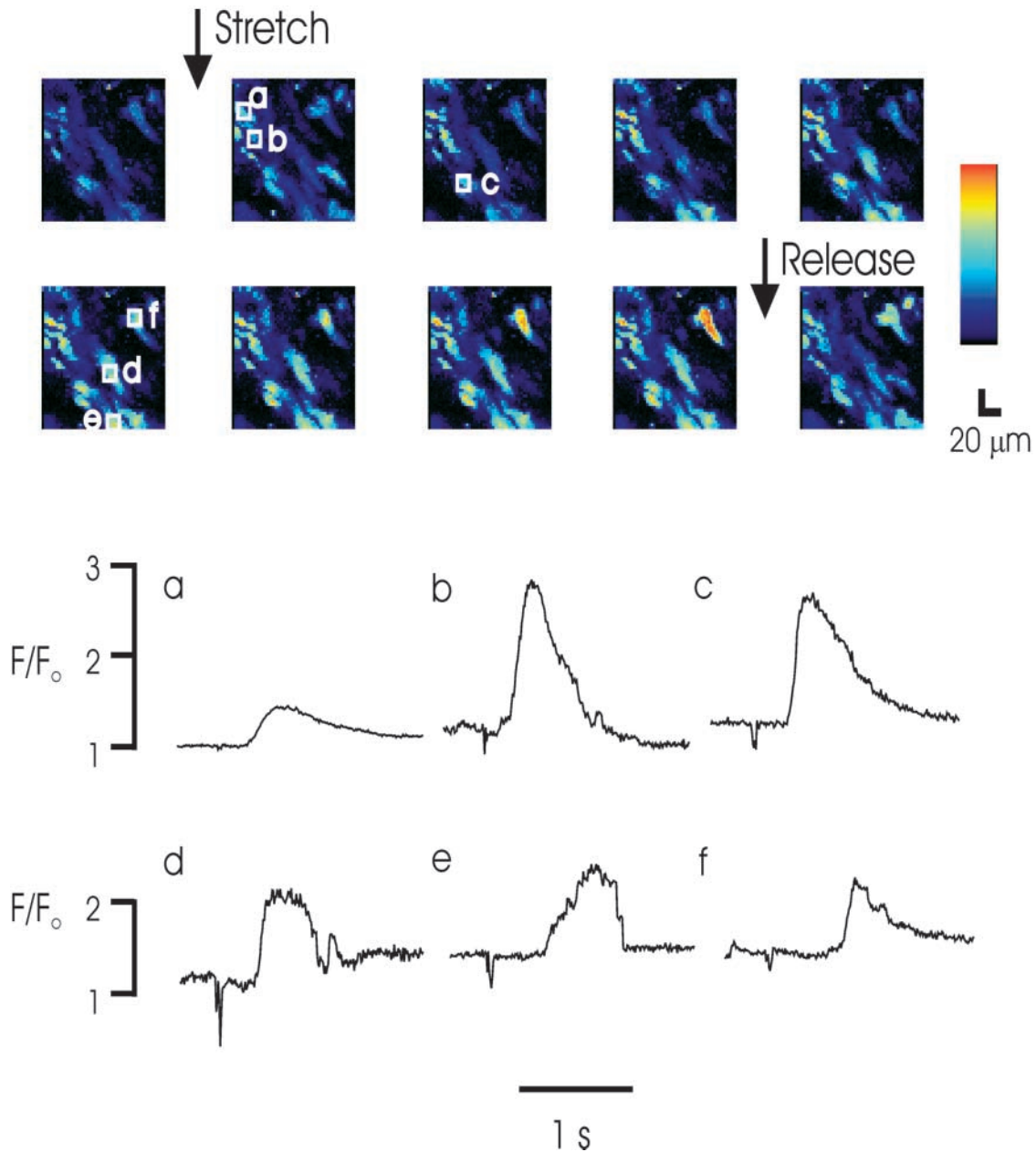
539   JI ET AL.

FIGURE 6. Stretch-induced Ca^{2+} waves in intact mouse urinary bladder smooth muscle tissue. Above, images from a confocal time series obtained at 57.3-ms intervals. Individual boxed cell areas identify regions for which fluorescent profiles are shown below. A motion artifact identifies the point of tissue stretch on the fluorescent profiles. Note the wave of calcium evoked in single cells as the tissue is stretched. The full time series indicates evoked Ca^{2+} waves within individual cells that are not transmitted to neighboring cells. Pixel size = 2.35 µM.

(STICs) (Wang et al., 1992; Janssen and Sims, 1994), to larger currents with a timecourse equivalent to the underlying Ca^{2+} waves. Stretch-activated STICs were observed in 6 out of 11 mouse and 6 out of 10 rabbit cells. Fig. 5 A shows the fluorescence magnitude from the area of a cell in which a Ca^{2+} spark was recorded, and the simultaneously recorded transient current, demonstrating the superposition of these events. Moreover, as shown in Fig. 5 A, stretch-activated chloride currents were equivalent in the presence of 50 µM Gd^{3+}, which blocks these currents in guinea pig bladder urinary myocytes (Wellner and Isenberg, 1993a). STICs were observed in four out of eight such experiments (3/5 rabbit and 1/3 mouse cells). Moreover, in this experiment Gd^{3+} was present to block activation of stretch-induced currents. In some experiments, STICs were observed before and after the stretch events, and the frequency of equivalent STICs increased markedly during cell stretch. As shown in Fig. 5 B, the amplitude and kinetics of currents trig-

gered by increases in cell length was equivalent to spontaneous events observed before cell stretch.

Voltage ramps and step protocols employed during activation of the current indicated that the reversal potential in physiological salt solution was ∼0 mV ($n = 7$). Partial replacement of chloride with glutamate ions (100 mM NaGlutamate substituted for NaCl) shifted the reversal potential to 18 ± 3.2 mV ($n = 7$; Fig. 5 C), close to the theoretical chloride reversal potential of 24 mV, indicating that the currents were anion selective, consistent with the opening of calcium-activated chloride currents, rather than stretch-activated cation currents. Using increases of cell length of ∼20%, we did not observe stretch-activated cation currents in whole-cell recordings of rabbit or mouse bladder myocytes, and the current reversal potential of stretch-activated chloride currents was not altered by inclusion of Gd^{3+} in the external solution.

Stretch-induced Ca^{2+} Sparks and Ca^{2+} Waves in Intact Smooth Muscle Tissue

If SICR is a physiological component of Ca^{2+} regulation in smooth muscle, the phenomenon should be observed in multicellular preparations. Such a demonstration would also rule out the possibility that SICR is an epiphenomenon associated with single myocytes and possible damage associated with enzymatic dissociation. We therefore examined SICR in intact mouse urinary bladder segments suspended between T-shaped aluminum clips on a micromanipulator. Loading of Fluo-4 was facilitated by brief (5 min) incubation of the tissue with collagenase (see MATERIALS AND METHODS). An example of a typical experiment in which a muscle segment was stretched from resting length is shown in Fig. 6. Serial high speed confocal images revealed sparks and Ca^{2+} waves in most cells in muscle segments following passive stretch of the tissue. Ca^{2+} waves were observed to propagate intracellularly, but not intercellularly in these experiments.

DISCUSSION

The release of free Ca^{2+} ions from the sarcoplasmic reticulum is a fundamental event in muscle contraction and an array of biochemical and allosteric mechanisms have evolved to link intracellular Ca^{2+} release channels with extracellular signals transduced at the sarcolemma. Unlike sarcomeric muscle, which responds to a relatively limited set of inputs, smooth muscle subserves diverse functions and, not surprisingly, the tissue displays a correspondingly complex array of Ca^{2+} mobilization processes. Thus, a highly developed $InsP_3$ receptor system mediates slow and sustained Ca^{2+} release following the binding of hormones or autocoids to cognate receptors (Baron et al., 1984; Somlyo et al., 1985).

Ca^{2+}-permeant sarcolemmal ion channels that are both voltage- and ligand-gated allow direct influx of Ca^{2+} ions to the cytosol (Benham et al., 1985, 1987; Nelson et al., 1988), and RYRs, which play a dominant role in sarcomeric muscle excitation-contraction coupling, are spontaneously active in many smooth muscles (Nelson et al., 1995; ZhuGe et al., 1998) and are activated following the opening of L-type Ca^{2+} channels during the action potential (Imaizumi et al., 1998; Collier et al., 1999). Here, we have expanded the set of signals known to trigger Ca^{2+} to include stretch of the sarcolemma, resulting in SICR. We have shown that this mechanical stimulus results in gating of RYR in a manner that is independent of the gating of stretch-activated channels or a rise in $[Ca^{2+}]_i$ (Figs. 1, 3, and 4); that the process results in the release of unitary Ca^{2+} sparks at predictable regions within a cell known as frequent discharge sites (Bolton and Gordienko, 1998) or leads to a wave of Ca^{2+} release that is transmitted through the cytosol and coupled to the activation of calcium-activated membrane ion channels (Figs. 1 and 5); that there is an intrinsic desensitization to the process, resulting in a prominent accommodation to changes in cell length (Fig. 2); and that the process occurs in smooth muscle in situ (Fig. 6).

These findings may be viewed in the context of recent demonstrations of mechanically induced increases in $[Ca^{2+}]_i$ in single cells (Niggel et al., 2000). Using collagen-coated magnetite particles, Niggel et al. (2000) demonstrated a transient rise in $[Ca^{2+}]_i$ in astrocytes, endothelial cells, and glioma cells in tissue culture. In several, but not all, experiments, this Ca^{2+} release occurred in the absence of extracellular Ca^{2+}, similar to our findings. Interestingly, Ca^{2+} release in some cells was inhibited by xestospongin, suggesting activation of $InsP_3$ receptor–mediated Ca^{2+} release. Stretch-dependent Ca^{2+} release has also been demonstrated recently in cardiac muscle (Petroff et al., 2001). In this study, spontaneous Ca^{2+} sparks were observed to increase in frequency in ventricular myocytes following mechanical elongation. As in smooth muscle, the increase in cardiac Ca^{2+} sparks was not associated with stretch-activated ion influx, but was shown to involve the generation of nitric oxide. Together, these studies suggest that multiple stretch-induced Ca^{2+} release pathways may exist, and lend support for the demonstration of a SICR mechanism that is independent of a rise in $[Ca^{2+}]_i$.

One important unresolved issue in smooth muscle is the nature of the process or processes regulating so called "spontaneous" calcium release events (Benham and Bolton, 1986). Our results suggest that one element in this regulation may be the degree of stretch of the myocyte membrane: small increases in the length of myocytes within muscles could result in transient Ca^{2+} release. Although Ca^{2+} release appears to desensi-

tize over time at any given level of cell length (Fig. 2), additional step length changes result in further Ca^{2+} release. This could result in coupling between myocytes within contracting tissue: mechanical linkage of myocytes within a muscle would be expected to result in contraction of one region of a muscle causing an increase length of neighboring cells, with attendant Ca^{2+} release. Depending on the expression of calcium-activated potassium and calcium-activated chloride channels, and the cell membrane potential, the result would be a hyperpolarizing or depolarizing stimulus. Similarly, increases or decreases in cell length associated with changes in luminal pressure in vessels and hollow organs might be expected to affect Ca^{2+} release and result in coordinated changes in electrical activity. Recent data in which intravascular pressure and $[Ca^{2+}]_i$ have been simultaneously recorded are in general consistent with the release of $[Ca^{2+}]_i$ during increases in transmural pressure (Jaggar, 2001). In that study, elevations of vascular pressure increased Ca^{2+} spark frequency and evoked Ca^{2+} waves. Although this effect was abolished by diltiazem and interpreted to be a result of pressure-induced gating of L-type Ca^{2+} channels, the data are also consistent with pressure-induced gating of RYR, resulting in depolarization through calcium-sensitive conductances and activation of L-type channels.

The mechanism by which RYR channels are gated by stretch is unclear. Despite previous reports of stretch-induced cation currents in guinea pig urinary bladder myocytes (Kirber et al., 1988), we were unable to observe these currents in rabbit or mouse myocytes, and Ca^{2+} release occurred under conditions in which such currents would not be active (Ca^{2+}-free or Gd^{3+} external solutions). Moreover, our data indicate that a rise in $[Ca^{2+}]_i$ is not required in this process, thereby raising the possibility that SICR occurs by a mechanism quite separate from CICR, and perhaps analogous to the allosteric gating of type 1 RYR in skeletal muscle. This could be envisaged as an interaction between structural elements within the myoplasm and RYR. However, an attractive alternative hypothesis is that increases in cell length result in a more favorable arrangement of RYR, such that stochastic Ca^{2+} release from the SR results in the activation of sufficient RYR to generate a resolvable Ca^{2+} spark, whereas in the absence of close coupling between RYR, such stochastic events remain below the threshold of resolution. It would be difficult to rule out this hypothesis experimentally, as addition of mobile buffer would not be expected to disrupt such local coupling. There is experimental evidence both for the coupled gating of RYR (Stern et al., 1999; Marx et al., 2001) for such a process in striated muscle and for the importance of spatial ordering of individual elements within the "calcium release units" (Protasi et al., 1998; Franzini-Armstrong et al., 1999) influence of muscle

length on SR. It is difficult to imagine that this model could adequately explain the data in Fig. 2, however, where SICR occurs with additional lengthening following desensitization of SICR from a previous stretch. Rather, while the two above mechanisms need not be mutually exclusive (increases in cell length could result in RYR gating, which might then be more efficiently coupled at lengths above slack length) it seems that the most likely mechanism underlying SICR is through an effect on RYR gating. Additionally, it appears that either an intrinsic process of channel inactivation, or an adaptation to the mechanical stimulus, is required to explain the prominent desensitization that occurs at a given length.

In summary, we have identified a process of SICR from RYR. In smooth muscle cells, SICR appears to release Ca^{2+} repeatedly from the same sites, and these appear to be identical to those from which spontaneous Ca^{2+} sparks occur. The process does not require the gating of a sarcolemmal ion channel, nor a detectable rise in $[Ca^{2+}]_i$. It will be interesting to determine the extent to which this process occurs in other cells and tissues, and the coupling mechanism between sarcolemmal stretch and RYR gating.

REFERENCES

Baron, C.B., M. Cunningham, J.F. Strauss, III, and R.F. Coburn. 1984. Pharmacomechanical coupling in smooth muscle may involve phosphatidylinositol metabolism. *Proc. Natl. Acad. Sci. USA.* 81:6899–6903.

Bayliss, W.M. 1902. On the local reactions of the arterial wall to changes of internal pressure. *J. Physiol.* 28:220–231 (Abstr.).

Benham, C.D., and T.B. Bolton. 1986. Spontaneous transient outward currents in single visceral and vascular smooth muscle cells of the rabbit. *J. Physiol.* 381:385–406.

Benham, C.D., T.B. Bolton, N.G. Byrne, and W.A. Large. 1987. Action of externally applied adenosine triphosphate on single smooth muscle cells dispersed from rabbit ear artery. *J. Physiol.* 387:473–488.

Benham, C.D., T.B. Bolton, and R.J. Lang. 1985. Acetylcholine activates an inward current in single mammalian smooth muscle cells. *Nature.* 316:345–347.

Berridge, M.J. 1997. Elementary and global aspects of calcium signalling. *J. Exp. Biol.* 200:315–319.

Bolton, T.B., and D.V. Gordienko. 1998. Confocal imaging of calcium release events in single smooth muscle cells. *Acta Physiol. Scand.* 164:567–575.

Cannell, M.B., H. Cheng, and W.J. Lederer. 1995. The control of calcium release in heart muscle. *Science.* 268:1045–1049.

Collier, M.L., G. Ji, Y. Wang, and M.I. Kotlikoff. 2000. Calcium-induced calcium release in smooth muscle: loose coupling between the action potential and calcium release. *J. Gen. Physiol.* 115:653–662.

Collier, M.L., A.P. Thomas, and J.R. Berlin. 1999. Relationship between L-type Ca2+ current and unitary sarcoplasmic reticulum Ca2+ release events in rat ventricular myocytes. *J. Physiol.* 516: 117–128 (In Process Citation).

Fabiato, A. 1983. Calcium-induced release of calcium from the cardiac sarcoplasmic reticulum. *Am. J. Physiol.* 245:C1–C14.

Franzini-Armstrong, C., F. Protasi, and V. Ramesh. 1999. Shape, size, and distribution of Ca(2+) release units and couplons in skeletal and cardiac muscles. *Biophys. J.* 77:1528–1539.

Ganitkevich, V.Y., and G. Isenberg. 1992. Contribution of Ca(2+)-induced Ca2+ release to the [Ca2+]i transients in myocytes from guinea-pig urinary bladder. *J. Physiol.* 458:119–137.

Gordienko, D.V., T.B. Bolton, and M.B. Cannell. 1998. Variability in spontaneous subcellular calcium release in guinea-pig ileum smooth muscle cells. *J. Physiol.* 507:707–720.

Gordienko, D.V., I.A. Greenwood, and T.B. Bolton. 2001. Direct visualization of sarcoplasmic reticulum regions discharging Ca(2+)sparks in vascular myocytes. *Cell Calcium.* 29:13–28.

Guharay, F., and F. Sachs. 1984. Stretch-activated single ion channel currents in tissue-cultured embryonic chick skeletal muscle. *J. Physiol.* 352:685–701.

Imaizumi, Y., Y. Torii, Y. Ohi, N. Nagano, K. Atsuki, H. Yamamura, K. Muraki, M. Watanabe, and T.B. Bolton. 1998. Ca2+ images and K+ current during depolarization in smooth muscle cells of the guinea-pig vas deferens and urinary bladder. *J. Physiol.* 510: 705–719.

Jaggar, J.H. 2001. Intravascular pressure regulates local and global Ca(2+) signaling in cerebral artery smooth muscle cells. *Am. J. Physiol. Cell Physiol.* 281:C439–C448.

Janssen, L.J., and S.M. Sims. 1994. Spontaneous transient inward currents and rhythmicity in canine and guinea-pig tracheal smooth muscle cells. *Pflugers Arch.* 427:473–480.

Kirber, M.T., A. Guerrero-Hernandez, D.S. Bowman, K.E. Fogarty, R.A. Tuft, J.J. Singer, and F.S. Fay. 2000. Multiple pathways responsible for the stretch-induced increase in Ca2+ concentration in toad stomach smooth muscle cells. *J. Physiol.* 524:3–17.

Kirber, M.T., J.V.J. Walsh, and J.J. Singer. 1988. Stretch-activated ion channels in smooth muscle: a mechanism for the initiation of stretch-induced contraction. *Pflugers Arch.* 412:339–345.

Klein, M.G., H. Cheng, L.F. Santana, Y.H. Jiang, W.J. Lederer, and M.F. Schneider. 1996. Two mechanisms of quantized calcium release in skeletal muscle. *Nature.* 379:455–458.

Lipp, P., and E. Niggli. 1996. Submicroscopic calcium signals as fundamental events of excitation—contraction coupling in guinea-pig cardiac myocytes. *J. Physiol.* 492:31–38.

Lopez-Lopez, J.R., P.S. Shacklock, C.W. Balke, and W.G. Wier. 1995. Local calcium transients triggered by single L-type calcium channel currents in cardiac cells. *Science.* 268:1042–1045.

Marx, S.O., J. Gaburjakova, M. Gaburjakova, C. Henrikson, K. Ondrias, and A.R. Marks. 2001. Coupled gating between cardiac calcium release channels (ryanodine receptors). *Circ. Res.* 88:1151–1158.

Nabauer, M., G. Callewaert, L. Cleemann, and M. Morad. 1989. Regulation of calcium release is gated by calcium current, not gating charge, in cardiac myocytes. *Science.* 244:800–803.

Nakai, J., N. Sekiguchi, T.A. Rando, P.D. Allen, and K.G. Beam. 1998. Two regions of the ryanodine receptor involved in coupling with L-type Ca2+ channels. *J. Biol. Chem.* 273:13403–13406.

Nelson, M.T., H. Cheng, M. Rubart, L.F. Santana, A.D. Bonev, H.J. Knot, and W.J. Lederer. 1995. Relaxation of arterial smooth muscle by calcium sparks. *Science.* 270:633–637.

Nelson, M.T., N.B. Standen, J.E. Brayden, and J.F. Worley. 1988. Noradrenaline contracts arteries by activating voltage-dependent calcium channels. *Nature.* 336:382–385.

Niggel, J., W. Sigurdson, and F. Sachs. 2000. Mechanically induced calcium movements in astrocytes, bovine aortic endothelial cells and C6 glioma cells. *J. Membr. Biol.* 174:121–134.

Petroff, M.G., S.H. Kim, S. Pepe, C. Dessy, E. Marban, J.L. Balligand, and S.J. Sollott. 2001. Endogenous nitric oxide mechanisms mediate the stretch dependence of Ca2+ release in cardiomyocytes. *Nat. Cell Biol.* 3:867–873.

Protasi, F., C. Franzini-Armstrong, and P.D. Allen. 1998. Role of ryanodine receptors in the assembly of calcium release units in skeletal muscle. *J. Cell Biol.* 140:831–842.

Sigurdson, W., A. Ruknudin, and F. Sachs. 1992. Calcium imaging of mechanically induced fluxes in tissue-cultured chick heart: role of stretch-activated ion channels. *Am. J. Physiol.* 262:H1110–H1115.

Somlyo, A.P., J.W. Walker, Y.E. Goldman, D.R. Trentham, S. Kobayashi, T. Kitazawa, and A.V. Somlyo. 1988. Inositol trisphosphate, calcium and muscle contraction. *Philos. Trans. R. Soc. Lond. B Biol. Sci.* 320:399–414.

Somlyo, A.V., M. Bond, A.P. Somlyo, and A. Scarpa. 1985. Inositol trisphosphate-induced calcium release and contraction in vascular smooth muscle. *Proc. Natl. Acad. Sci. USA.* 82:5231–5235.

Stern, M.D., L.S. Song, H. Cheng, J.S. Sham, H.T. Yang, K.R. Boheler, and E. Rios. 1999. Local control models of cardiac excitation-contraction coupling. A possible role for allosteric interactions between ryanodine receptors. *J. Gen. Physiol.* 113:469–489.

Tanabe, T., K.G. Beam, B.A. Adams, T. Niidome, and S. Numa. 1990. Regions of the skeletal muscle dihydropyridine receptor critical for excitation-contraction coupling. *Nature.* 346:567–569.

Tanabe, T., K.G. Beam, J.A. Powell, and S. Numa. 1988. Restoration of excitation-contraction coupling and slow calcium current in dysgenic muscle by dihydropyridine receptor complementary DNA. *Nature.* 336:134–139.

Wang, Q., R.C. Hogg, and W.A. Large. 1992. Properties of spontaneous inward currents recorded in smooth muscle cells isolated from the rabbit portal vein. *J. Physiol.* 451:525–537.

Wellner, M.C., and G. Isenberg. 1993a. Properties of stretch-activated channels in myocytes from the guinea-pig urinary bladder. *J. Physiol.* 466:213–227.

Wellner, M.C., and G. Isenberg. 1993b. Stretch-activated nonselective cation channels in urinary bladder myocytes: importance for pacemaker potentials and myogenic response. *EXS.* 66:93–99.

Wellner, M.C., and G. Isenberg. 1994. Stretch effects on whole-cell currents of guinea-pig urinary bladder myocytes. *J. Physiol.* 480: 439–448.

ZhuGe, R., S.M. Sims, R.A. Tuft, K.E. Fogarty, and J.V. Walsh, Jr. 1998. Ca2+ sparks activate K+ and Cl− channels, resulting in spontaneous transient currents in guinea-pig tracheal myocytes. *J. Physiol.* 513:711–718.